Pourmohamadian, H., *et al.*: Investigating the Effect of Brownian Motion Models on ...
THERMAL SCIENCE: Year 2019, Vol. 23, No. 2A, pp. 485-496

485

INVESTIGATING THE EFFECT OF BROWNIAN MOTION MODELS ON HEAT TRANSFER AND ENTROPY GENERATION IN NANOFLUID FORCED CONVECTION

by

Hossein POURMOHAMADIAN[a], Ghanbar Ali SHEIKHZADEH[b], Alireza AGHAEI[c], Hamidreza EHTERAM[b], and Mohammad ADIBI[b]*

[a] Department of Engineering, Naragh Branch, Islamic Azad University, Naragh, Iran
[b] Faculty of Mechanical Engineering, University of Kashan, Kashan, Iran
[c] Young Researchers and Elite Club, Arak Branch, Islamic Azad University, Arak, Iran

In this study the influence of Brownian motion models on fluid-flow, heat transfer, and entropy generation in nanofluid forced convection with variable properties has been numerically inspected in a enclosure with central heat source. The governing equations were solved by finite volume method and SIMPLER algorithm. The numerical study was carried out for Reynolds numbers between 10 and 1000 and nanoparticles volume fraction between 0 and 0.04. The numerical results show that for all investigated models the average Nusselt number increases by nanoparticle volume fraction increment in all Reynolds number. The overall entropy generation behavior is similar to average Nusselt number variation for all inspected models. Among all analyzed models the estimation of Maxwell-Brinkman and Das-Vajjha are mainly closed to each other.

Key words: *nanofluid, Brownian motion, entropy, heat source, numerical study, forced convection*

Introduction

In 1995 Stephen Choi was the first person who used *nanofluid* term for nanoparticles suspensions in liquid in Argon laboratory and claimed that these fluids are totally different with common suspensions of solid-liquid and macro fluids in the case of preparation and stability and transient properties [1]. Nanofluid can be used in wide range of applications like industry, installation and other different branches such as medicine. Forced convection has a lot of usages in electronic, food industry, nuclear reactors, industrial lubrication, solar pools, solar collectors, heat exchangers, metal foundries, glassblowing, and other things. The entropy generation indicates the amount of irreversibility in a process and furthermore it can be a criterion for engineering system performance [2]. Minimizing the entropy generation or thermo- dynamical optimization is not an old method and it is a part of exergy analysis [3]. Sunder and Sharma [4], investigated numerically the water-Al_2O_3 nanofluid forced convection heat transfer in low volume fractions in a channel with heated walls. Based on their results the average Nusselt number increases according to nanoparticles volume fraction and it decreases by increasing the aspect ratio that is defined as ratio of width to height. Maruji and Razvarz [5], empirically analyzed the nanofluid forced convection heat transfer in a fully developed region of a pipe with

---

constant heat flux. Depending on their results the convective heat transfer coefficient increases by increasing Reynolds number but this increased value is dependent on length to diameter ratio. Maruji *et al.* [6], numerically inspected the nanofluid forced convective heat transfer with non-Newtonian behavior consideration. They presented their results in the case of a correlation for Nusselt number according to Reynolds and Prantdl numbers, volume fraction, and viscosity. Recently very numerically study conducted for the effect of the viscosity and thermal conductivity on the heat ransfer of nanofluid [7-20]. Pakravan and Yaghubi [21], analyzed the dufour, thermophoresis and Brownian effect in natural convection of water-SiO$_2$, water-CuO, and water-TiO nanofluids. They found out that the combined effect of these three parameters on average Nusselt number is substantially dependent on the investigated geometry. They reported that the average Nusselt number decreases by increasing the nanoparticles volume fraction inside the square enclosure. Arefmanesh *et al.* [22], employing different thermal conductivity and viscosity models for the CuO-water nanofluid, occupying a lid-driven trapezoidal enclosure, on the fluid-flow and heat transfer within the enclosure have been investigated numerically. Results indicate that, for constant values of Ri and ϕ, the differences between the streamlines as well as between the isotherms obtained by employing the five different models are insignificant. Hadad and Abu-Nada [23], studied the thermophoresis effects and Brownian motion in natural convection numerically. Their results indicated that the heat transfer increases by considering the thermophoresis effect and Brownian motion for all volume fractions. Besides this increase is more substantial in low volume fractions. Seif and Nikaien [24], investigated the forced convection of CuO, Al$_2$O$_3$, and ZnO with EG-water base fluid inside the heat sink micro channel numerically. They demonstrated that the Brownian motion effect is more for nanofluids with smaller nanoparticles. Bianco *et al.* [25, 26] investigated the production of nanoparticle entropy of Al$_2$O$_3$ in a tube. Based on their results, with increasing volume fraction of nanoparticles, the production entropy also increases.

The investigations show that more investigations in this field are required. One of the reasons for the inconsistency of experimental results with numerical studies is not to consider some of the important effects, such as the browning of nanoparticles. In this study, we tried to obtain more accurate numerical results considering the effect of this motion. The investigations have been carried out so far, researchers have not studied the effect of Brownian's motion on forced convection. This geometry can be an example of CPU cooling of a powerful computer. These kinds of computers have the ability to process a lot of data at a low cost. For this reason CPU of computers generate a lot of heat. Using nanofluids can be a suggestion for more efficient cooling of these systems. Another idea is the proposed geometry for the photovoltaic cooling system. In this study, the effect of Brownian motion with the help of three different models on the flow field, heat transfer, and production of entropy of Cu-water-boron nanoparticles in compulsory convection is investigated. Study for volume fractions of 0-4% of nanoparticles and Reynolds numbers from 10-1000 is done.
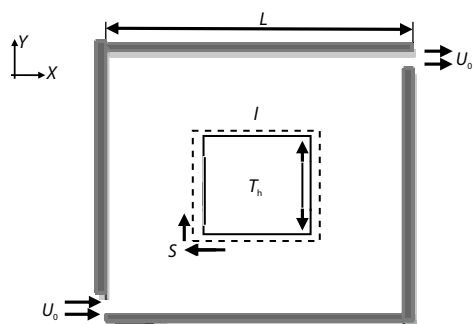
Problem geometry

The schematic geometry of the problem has been shown in fig. 1. The entrance and exit length region of the nanofluid is $L/10$ in the vertical walls. The thermal source is in constant

Figure 1. The schematic diagram of problem and boundary conditions

temperature, T_h, and the walls are insulated. The s distance that is calculated from the corner of the thermal source has been demonstrated in fig. 1. The nanofluid flow is laminar, steady and incompressible. The study has been conducted for Reynolds numbers of 10, 50, 100, 500, and 1000 and nanoparticles volume fraction between 0 and 0.04 with three different models for viscosity and thermal conductivity, [27-30].

Table 1. The base fluid thermophysical properties ($T = 300$ K) and nanoparticles [18]

Properties	CuO	Water
C_p [Jkg^{-1}K^{-1}]	535.6	4179
ρ [kgm^{-3}]	6320	997.1
k [Wm^{-1}K^{-1}]	76.5	0.613
β [K^{-1}]	$1.8 \cdot 10^{-5}$	$21 \cdot 10^{-5}$
μ [Wm^{-1}K^{-1}]	–	0.001003

Nanofluid properties

The thermophysical properties of water as a base fluid are presented in tab. 1 [18].

Governing equations

The governing equations including continuity, momentum, and energy equations for Newtonian fluid, 2-D flow, laminar, steady are defined below:

$$\frac{\partial u}{\partial x} + \frac{\partial v}{\partial y} = 0 \tag{1}$$

$$u\frac{\partial u}{\partial x} + v\frac{\partial u}{\partial y} = -\frac{1}{\rho_{nf}}\frac{\partial p}{\partial x} + \frac{1}{\rho_{nf}}\left[\frac{\partial}{\partial x}\left(\frac{\mu_{nf}\partial u}{\partial x}\right) + \frac{\partial}{\partial y}\left(\frac{\mu_{nf}\partial u}{\partial y}\right)\right] \tag{2}$$

$$u\frac{\partial v}{\partial x} + v\frac{\partial v}{\partial y} = -\frac{1}{\rho_{nf}}\frac{\partial p}{\partial y} + \frac{1}{\rho_{nf}}\left[\frac{\partial}{\partial x}\left(\frac{\mu_{nf}\partial v}{\partial x}\right) + \frac{\partial}{\partial y}\left(\frac{\mu_{nf}\partial v}{\partial y}\right)\right] \tag{3}$$

$$u\frac{\partial T}{\partial x} + v\frac{\partial T}{\partial y} = \frac{1}{(\rho C_p)_{nf}}\left[\frac{\partial}{\partial x}\left(k_{nf}\frac{\partial T}{\partial x}\right) + \frac{\partial}{\partial y}\left(k_{nf}\frac{\partial T}{\partial y}\right)\right] \tag{4}$$

$$S_{gen} = \frac{k_{nf}}{T_0^2}\left[\left(\frac{\partial T}{\partial x}\right)^2 + \left(\frac{\partial T}{\partial y}\right)^2\right] + \frac{\mu_{nf}}{T_0}\left[2\left(\frac{\partial u}{\partial x}\right)^2 + 2\left(\frac{\partial v}{\partial y}\right)^2 + \left(\frac{\partial u}{\partial y} + \frac{\partial v}{\partial x}\right)^2\right] \tag{5}$$

The non-dimensional parameters used in mixed convection are introduced in correlation eq. (6):

$$X = \frac{x}{L}, \ Y = \frac{y}{L}, \ V = \frac{v}{U_0}, \ U = \frac{u}{U_0}, \ \theta = \frac{T-T_c}{\Delta T}, \ P = \frac{p}{\rho U_0^2},$$

$$T_0 = \frac{T_h + T_c}{2}, \ \Delta T = T_h - T_c, \ \text{Re} = \frac{U_0 L}{\nu_f}, \ \text{Pr} = \frac{\nu_f}{\alpha_f} \tag{6}$$

By using the non-dimensional parameters the non-dimensional equations of continuity, momentum and energy are obtained:

$$\frac{\partial U}{\partial X} + \frac{\partial U}{\partial Y} = 0 \tag{7}$$

$$U\frac{\partial U}{\partial X}+V\frac{\partial U}{\partial Y}=-\frac{\partial P}{\partial X}+\frac{1}{\rho_{nf}\nu_f \operatorname{Re}}\left[\frac{\partial}{\partial X}\left(\frac{\mu_{nf}\partial U}{\partial X}\right)+\frac{\partial}{\partial Y}\left(\frac{\mu_{nf}\partial U}{\partial Y}\right)\right] \tag{8}$$

$$U\frac{\partial V}{\partial X}+V\frac{\partial V}{\partial Y}=-\frac{\partial P}{\partial Y}+\frac{1}{\rho_{nf}\nu_f \operatorname{Re}}\left[\frac{\partial}{\partial X}\left(\frac{\mu_{nf}\partial V}{\partial X}\right)+\frac{\partial}{\partial Y}\left(\frac{\mu_{nf}\partial V}{\partial Y}\right)\right] \tag{9}$$

$$U\frac{\partial\theta}{\partial X}+V\frac{\partial\theta}{\partial Y}=\frac{1}{\operatorname{Re}\operatorname{Pr}\alpha_f(\rho c_p)_{nf}}\left[\frac{\partial}{\partial X}\left(\frac{k_{nf}\partial\theta}{\partial X}\right)+\frac{\partial}{\partial Y}\left(\frac{k_{nf}\partial\theta}{\partial Y}\right)\right] \tag{10}$$

$$S_{\text{gen}}=\frac{k_{nf}}{k_f}+\left[\left(\frac{\partial\theta}{\partial X}\right)^2+\left(\frac{\partial\theta}{\partial Y}\right)^2\right]+\chi\frac{\mu_{nf}}{\mu_f}\left[2\left(\frac{\partial U}{\partial X}\right)^2+2\left(\frac{\partial V}{\partial Y}\right)^2+\left(\frac{\partial U}{\partial Y}+\frac{\partial V}{\partial X}\right)^2\right] \tag{11}$$

According to the geometry, the boundary conditions are:

$$U=V=0,\ \theta=0\quad\text{on heat source}\quad U=V=0,\ \theta=1\quad\text{on all the outer walls} \tag{12}$$

The nanofluid properties including density, specific heat, thermal expansion, and diffusivity are obtained from eq. (13) to eq. (16):

$$\rho_{nf}=(1-\varphi)\rho_f+\varphi\rho_s \tag{13}$$

$$(\rho c_p)_{nf}=(1-\varphi)(\rho c_p)+\varphi(\rho c_p)_s \tag{14}$$

$$(\rho\beta)_{nf}=(1-\varphi)(\rho\beta)_f+\varphi(\rho\beta)_s \tag{15}$$

$$\alpha_{nf}=\frac{k_{nf}}{(\rho c_p)_{nf}} \tag{16}$$

Viscosity and thermal conductivity calculation

In this section the viscosity and thermal conductivity correlations in different models are presented.in Maxwell-Brinkman model the viscosity [27] and thermal conductivity [28] that are only functions of nanoparticles volume fractions are obtained from eqs. (17) and (18).

$$\mu_{nf}=\mu_f(1-\varphi)^{-2.5} \tag{17}$$

$$k_{nf}=k_f\left[\frac{(k_s+2k_f-2\varphi(k_f-k_s)}{(k_s+2k_f)+\varphi(k_f-k_s)}\right] \tag{18}$$

In Koo and Kleinstrener [29] and Vajjha and Das [30] viscosity and thermal conductivity are functions of nanoparticles volume fraction and temperature also the Brownian motion effect is considered for them. in these models viscosity and thermal conductivity are attained from correlations eqs.(17) and (18) and the Brownian part of thermal conductivity and viscosity are obtained from correlations eqs. (21) to (25) based on their models.

$$\mu_{nf}=\mu_{\text{static}}+\mu_{\text{Brownian}} \tag{19}$$

$$k_{nf}=k_{\text{static}}+k_{\text{Brownian}} \tag{20}$$

where $k_{Brownian}$ in Koo model is defined as [29]:

$$k_{Brownian} = 5 \cdot 10^4 \lambda \varphi \rho_f c_{p,f} \sqrt{\frac{\kappa T}{\rho_s d_p}} \xi(T, \varphi) \tag{21}$$

ρ_s and d_p ($d_p = 29 \cdot 10^{-9}$) are nanoparticles density and radius, respectively. For water-CuO nanofluid the λ and ξ functions that are estimated empirically are as follow for the range of $300 < T \, (K) < 325$, [29].

$$\lambda = 0.0137(100\varphi)^{-0.8229} \quad \text{for} \quad \varphi \leq 1\%, \quad \lambda = 0.0011(100\varphi)^{-0.7272} \quad \text{for} \quad \varphi > 1\%$$
$$\xi(T, \varphi) = (-6.04\varphi + 0.4705)T + (1722.3\varphi - 134.63) \quad \text{for} \quad 1\% \leq \varphi \leq 4\% \tag{22}$$

$k_{Brownian}$ in Vajjha and Das [30] is defined:

$$k_{Brownian} = 5 \cdot 10^4 \beta \varphi \rho_l c_{p,l} \sqrt{\frac{\kappa T}{2\rho_s R_s}} f(T, \varphi) \tag{23}$$

$$f(T, \varphi) = (2.8217 \cdot 10^{-2} \varphi + 3.917 \cdot 10^{-3}) \frac{T}{T_0} + (-3.0669 \cdot 10^{-2} \varphi - 3.91123 \cdot 10^{-3}) \tag{24}$$

where κ is the Boltzman constant ($\kappa = 1.3807 \cdot 10^{-23}$). The $\mu_{Brownian}$ in all models is defined:

$$\mu_{Brownian} = \frac{k_{Brownian}}{k_f} \frac{\mu_f}{Pr} \tag{25}$$

The Nusselt number on the hot wall is:

$$Nu_{avg} = \frac{1}{41} \int\limits_{on \, heat \, source \, walls} Nu \, dS \tag{26}$$

Numerical solution

The governing differential equations are solved by an appropriate numerical proce-dure. Hence the grid of nodes will be matched on the solution field and then by discretizing the equations on this grid these equations will be converted to algebraic equations in each point of this grid. In order to convert the differential equations to system of algebraic equation the finite volume method presented by Patankar [31] is used. The governing equations were solved by finite volume method and SIMPLER algorithm. Diffusion terms were solved by second order central difference and convective terms were discretized by Hy-brid method. Subsequently the system of equations was solved by iterative method.

The optimum grid

In order to find the appropriate grid that leads to result inde-pendence from grid, the average Nusselt number was calculated for CuO-water nanofluid for grids with different nodes, 61×61, 71×71, 81×81, 91×91, and 101×101 for Brinkman model, with Reynolds number of 100 and volume fraction of 0.02. The results were compared in tab. 2. It is obvious that the grid with 91×91 is appropriate based on average Nusselt number values.

Table 2. Average Nusselt number for Maxwell-Brinkman [27, 28] model, and for different nodes

Node numbers	Nu_{avg}
61×61	5.36
71×71	5.53
81×81	5.67
91×91	5.72
101×101	5.74

The convergence criterion for pressure, velocity, and temperature is obtained from eq. (27), that M and N are node numbers of the grid in *x*- and *y*-direction and ζ is the parameter that is solved. The *K* is the number of iterations and maximum error value is 10^{-6}:

$$\text{eror} = \frac{\sum_{i=1}^{M}\sum_{j=1}^{N}|\zeta_{i,j}^{K+1} - \zeta_{i,j}^{K}|}{\sum_{i=1}^{M}\sum_{j=1}^{N}|\zeta_{i,j}^{K+1}|} \leq 10^{-6} \tag{27}$$

Table 3. Comparison of average Nusselt number in mixed convection

Ri	φ	Present work	[32]	Difference percentage
0.01	0.02	33.14	32.80	1.04
	0.1	36.40	36.90	1.36
10	0.02	1.68	1.72	2.32
	0.1	1.93	2.01	3.98

Numerical program validation

In order to validate the results of provided computer program the numerical simulation was carried out and the obtained results were compared with the [32]. The numerical results with the present program and the attained results were compared with the results in tab. 3. relative difference between average Nusselt number values is insignificant as a consequence the validation of modeling results is proved.

Result and discussion

Vertical velocity component changes

The vertical velocity component change in the middle height based on *X*, in has been shown in fig. 2, this quantity can be a criterion for convection and nanofluid movement. In all three investigated models for Reynolds numbers of 10, 50, 100 the flow enters from left side of enclosure and moves toward the exit that is in the right side of the enclosure from top and bottom of heat source. It is evident from fig. 2 that the vertical component of velocity in two sides of heat source (where the velocity is zero) is positive and there is no difference in value between them. In Reynolds numbers of 500 and 1000 the velocity is negative in the left side of heat source and it is positive in the right side. The velocity value in the right side of heat source is much more than the velocity in the left side. Actually in Reynolds numbers of 500 and 1000 that the great part of flow has moved from bottom of the heat source and in the top part of the heat source that the vortexes move counter clockwise is formed. There is no considerable difference among investigated models in the case of vertical velocity component change and its value.
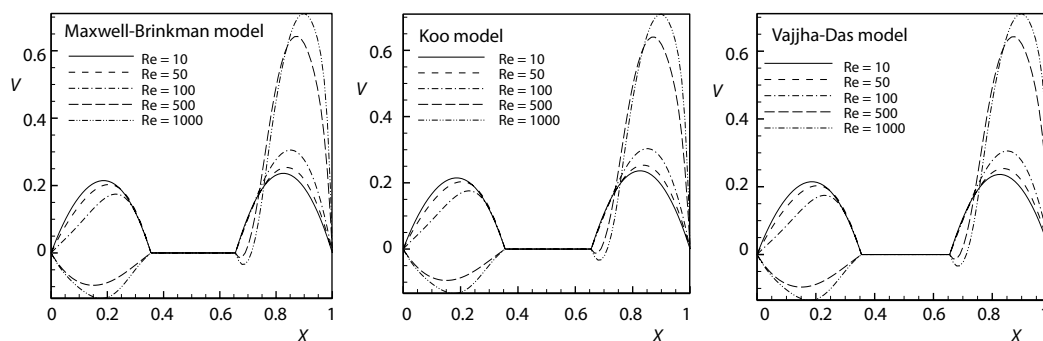

Figure 2. Vertical velocity component variation in the middle height based on *X*, and $\varphi = 0.02$

Pourmohamadian, H., *et al.*: Investigating the Effect of Brownian Motion Models on ...
THERMAL SCIENCE: Year 2019, Vol. 23, No. 2A, pp. 485-496

491

Temperature variations

The temperature variations have been shown in fig. 3 in the middle height based on X and, $\varphi = 0.02$. By increasing the Reynolds numbers the temperature in the entrance side and close to the heat source is less than the temperature in lower Reynolds numbers. On the other hand by Reynolds number increment the temperature gradient intensifies near the heat source. Among all investigated models except Reynolds number of ten the temperature variations are extremely intense in the right side of heat source and the temperature drops only after a short length and it reaches to nanofluid fluid temperature in the exit. For Reynolds numbers of 500 and 1000 the temperature variations in both sides of hat source is symmetric. For temperature variations there is no significant difference among various models like vertical velocity component change. In Reynolds of 100, close to left side of heat source the temperature variations are similar to Reynolds number of 10 and 50 and afterwards the temperature gradient intensifies substantially so that the temperature gradient gets even higher than the Reynolds numbers of 500 and 1000.
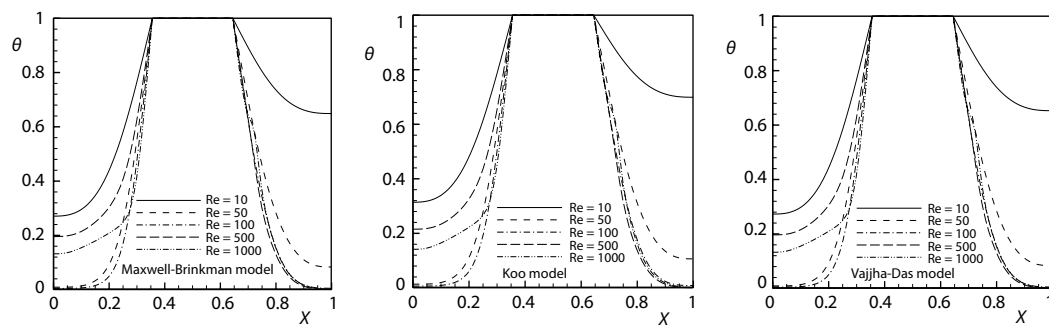

Figure 3. Temperature variation in the middle height based on X, and $\varphi = 0.02$

*Studying the stream
and isothermal lines*

The stream, isothermal and entropy lines are shown in fig. 4 for CuO-water nanofluids, in all Reynolds numbers and different models. The stream lines are dense in inlet and outlet of enclosure and in Reynolds numbers of 10, 50, and 100. These lines move toward the exit from both sides of heat source while for Reynolds numbers of 500 and 1000, the great part of flow has moved toward the exit, from bottom of the heat source in these Reynolds numbers a big vortex is formed in top part of enclosure around the heat source. This vortex moves counter clockwise in Reynolds numbers of 10 and 50 the stream line are in both sides of the enclosure in a symmetric shape while in Reynolds number of 100 the stream lines are not symmetric and the entrance region has a curve. In Reynolds numbers of 500 and 1000 some vortexes are formed in top and bottom corners of the enclosure. The stream lines are similar to in all investigated models. There is a slight difference between stream lines in Maxwell-Brinkman model comparing to two other temperature dependent models. For example in Maxwell-Brinkman model, the vortexes that are observed in bottom corner of the enclosure for Reynolds number of 1000 are bigger than the similar vortexes in temperature dependent models in Reynolds number of 10. The isothermal lines are dense in the bottom part of heat source. This compactness indicates more appropriate heat transfer in this region.
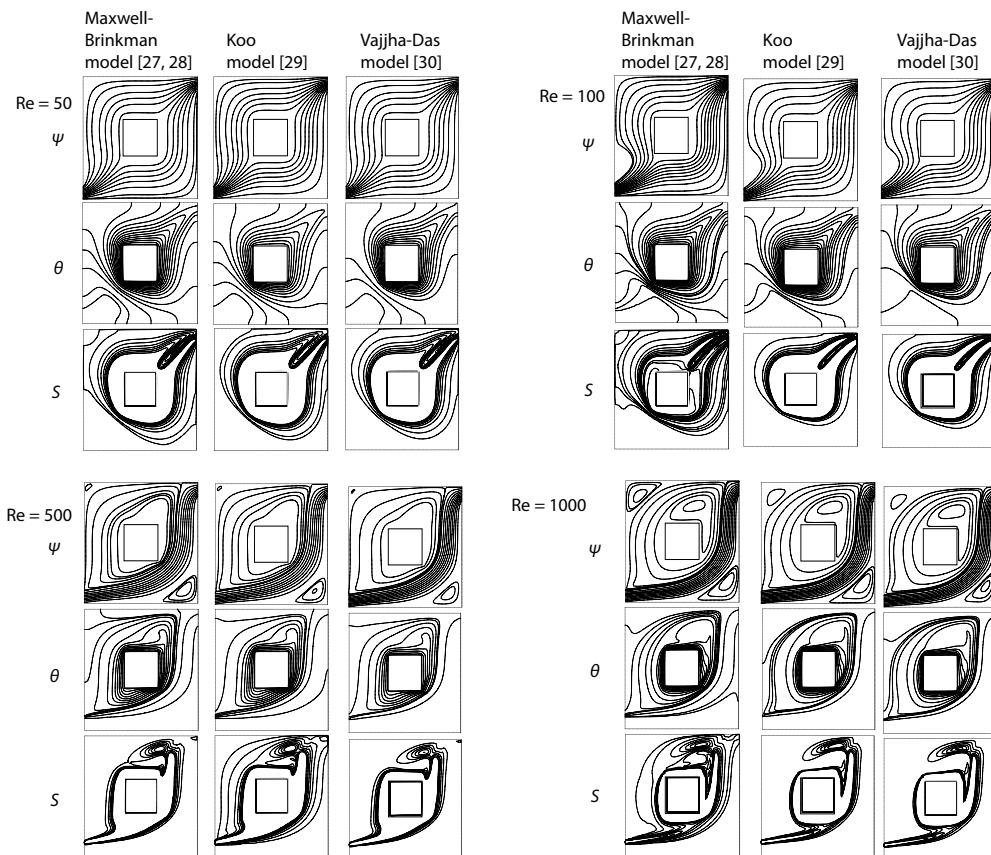
Figure 4. Stream lines, isothermal lines, and constant entropy lines in $\varphi = 0.02$ for different models and Reynolds numbers

Study of average Nusselt number variations

The average Nusselt number variations according to nanoparticles volume fractions have been demonstrated in fig. 5 for different models and Reynolds numbers.

Among all investigated Reynolds numbers the average Nusselt number increases by nanoparticles volume fraction increase. In fact by increasing nanoparticles volume fraction the
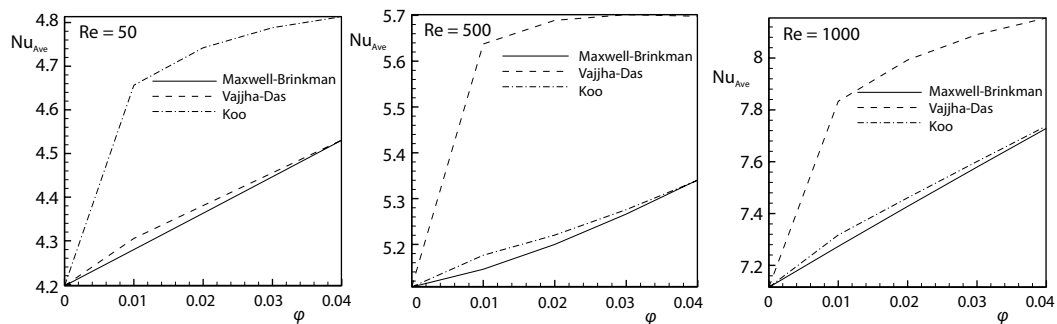

Figure 5. The average Nusselt number variations according to volume fraction for different models

Pourmohamadian, H., *et al.*: Investigating the Effect of Brownian Motion Models on ...
THERMAL SCIENCE: Year 2019, Vol. 23, No. 2A, pp. 485-496

493

nanofluid thermal conductivity increases hence the heat transfer increases. For all investigated models in a constant volume fraction the average Nusselt number increases by Reynolds number increment. In all analyzed Reynolds numbers the estimated average Nusselt numbers by Vajjha and Das [30] model is closed to predicted values by Maxwell-Brinkman model. These predictions for Nusselt number get closed to each other especially in volume fractions of 0.03 and 0.04. The maximum and minimum increase in average Nusselt number for Vajjha and Das [30] model comparing to Maxwell-Brinkman constant property model is 9.56% and 0.01% and they occur in Reynolds numbers of 500 and 50, with volume fractions of 0.01 and 0.04, respectively. In Koo [29] model the maximum and minimum increase in average Nusselt number comparing to Maxwell-Brinkman model is 8.82% and 3% and they occur in Reynolds numbers of 100 and 10, with volume fractions of 0.01 and 0.04, respectively.

The overall entropy generation variations according to Reynolds number

The overall entropy generation variations according to nanoparticles volume fraction are exhibited in fig. 6. The major part of entropy generation is due to heat for all investigated models. Consequently the entropy generation curves behavior is similar to average Nusselt number variations. The overall entropy generation increases by nanoparticles volume fraction increase. Nanoparticles volume fraction increase leads to more heat transfer, hence the entropy generation due to heat transfer increases. A great part of this entropy increase is due to enhancing heat transfer by Reynolds number increase and other part of that is increasing frictional loss by Reynolds number increment that results in frictional entropy increase. For Vajhha-Das model the max and min increase in overall entropy generation is 0.7% and 0.11% comparing to Maxwell-Brinkman constant property model and they occur in Reynolds numbers of 100 and 10, with volume fractions of 0.01 and 0.04, respectively. For Koo model the maximum and minimum increase in overall entropy generation is 10.11 and 1.07 comparing to Maxwell-Brinkman model and they occur in Reynolds numbers of 500 and 10, with volume fractions of 0.01 and 0.04, respectively.
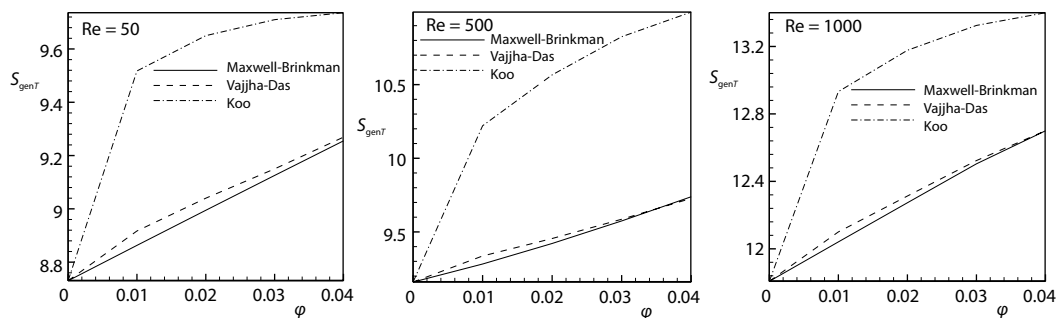

Figure 6. The overall entropy generation change according to nanoparticles volume fraction

Frictional entropy generation variations according to Reynolds number

The frictional entropy generation variations based on nanoparticles volume fractions have been depicted in fig. 7 for different Reynolds numbers and models. The generated entropy due to friction is insignificant and it is not more than 0.0001 % for all investigated cases and models. By increasing the nanoparticles volume fraction the frictional entropy generation increases. The nanoparticles volume fraction increase leads to nanofluid viscosity increment and
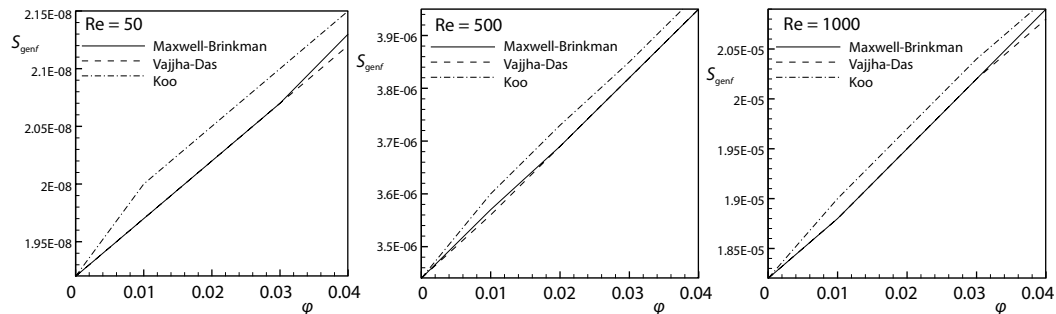
Figure 7. The variation of frictional entropy generation *vs*. volume fraction for different models

finally it enhances the frictional effects. In a constant volume fraction for all models the frictional entropy generation increases by Reynolds number. This is due to frictional effects increase caused by Reynolds number increase. The estimated values of frictional entropy by Vajjha-Das are really closed to the predicted values by Maxwell-Brinkman model.

This is due to closed estimation of nanofluid viscosity by these two models. For Vajjha and Das [30] model the maximum and minimum increase in frictional entropy generation is almost 0% in comparison with Maxwell-Brinkman constant property model. For Koo [29] model the maximum and minimum increase in frictional entropy generation is 1.82% and 0.67% in comparison with Maxwell-Brinkman model. Values occur in Reynolds numbers of 10 and 500, with volume fractions of 0.02 and 0.04, respectively. Given that the *k*-value predicted by the Vajjha-Das model is greater than the other models. The average Nusselt number predicted by this model is also larger and different than the other two models. There is also an argument for productive entropy.

Conclusions

In this study the numerical investigation of fluid-flow, heat transfer, and entropy generation of CuO-water nanofluid forced convection with variable properties have been implemented. The study was carried out for three models of Maxwell-Brinkman, Vajjha-Das, and Koo. In this section the obtained results are briefly presented as follows.

- By using the temperature dependent models to estimate the viscosity and thermal conductivity, the average Nusselt numbers and overall entropy generation are higher than the case with prediction of constant property model.
- For Vajjha-Das model the maximum and minimum increase in average Nusselt number were 9.56 and 0.01 in comparison with Maxwell-Brinkman constant property model. These values occur in Reynolds numbers of 500 and 50, with volume fractions of 0.01 and 0.04, respectively.
- For Koo model the maximum and minimum increase in average Nusselt number were 8.82%, and 3% in comparison with Maxwell-Brinkman model, in Reynolds numbers of 100 and 10 with volume fractions of 0.01 and 0.04, respectively.
- For Vajjha-Das model the maximum and minimum increase in overall entropy generation were 0.7 and 0.11 in comparison with Maxwell-Brinkman model. These values occur in Reynolds numbers of 100 and 10 and volume fractions of 0.01 and 0.04, respectively.
- For Koo model the maximum and minimum increase in overall entropy generation are 10.11 and 1.07 in comparison with Maxwell-Brinkman model. These values occur in Reynolds numbers of 50 and 10, with volume fractions of 0.01 and 004, respectively.

Pourmohamadian, H., *et al.*: Investigating the Effect of Brownian Motion Models on ...
THERMAL SCIENCE: Year 2019, Vol. 23, No. 2A, pp. 485-496

495

- The maximum and minimum increase in frictional entropy generation in Vajjha-Das model was almost zero percent in comparison with Maxwell-Brinkman model.
- In Koo model the maximum and minimum increase in frictional entropy generation were 1.82 and 0.67 in comparison with Maxwell-Brinkman model. These values occur in Reynolds numbers of 10 and 500, with volume fractions of 0.02 and 0.04.

References

[1] Ho, C. J., Chen, M. W., Numerical Simulation of Natural Convection of Nanofluid in a Square Enclosure: Effects Due to Uncertainties of Viscosity and Thermal Conductivity, *Int. J. Heat Mass Transfer*, *51* (2008), 17-18, pp. 4506-4516

[2] Cengel, Y. A., Boles, M. A., *Thermodynamics an Engineering Approach*, 5th ed., McGraw-Hill, New York, USA, 2006

[3] Rosen, M. A., Second-Law Analysis: Approach and Implications, *Int. J. of Energy Research*, *23* (1999), 5, pp. 415-429

[4] Sundar, S. L., Sharma, K. V., Heat Transfer Enhancements of Low Volume Concentration Al_2O_3 Nanofluid with Longitudinal Strip Inserts in a Tube, *Int. J. of Heat and Mass Transfer*, *53* (2010), 19-20, pp. 4280-4286

[5] Moraveji, M. K., Razvarz, S., Experimental Investigation of Aluminum Oxide Nanofluid on Heat Pipe Thermal Performance, *Int. Com. Heat and Mass Transfer*, *39* (2012), 9, pp. 1444-1448

[6] Moraveji, M. K., *et al.*, Modeling of Forced Convective Heat Transfer of a Non-Newtonian Nanofluid in the Horizontal Tube under Constant Heat Flux with Computational Fluid Dynamics, *International Communications in Heat and Mass Transfer*, *39* (2012), 7, pp. 995-999

[7] Yang, C., *et al.*, Convective Heat Transfer of Nanofluids in a Concentr ic Annulus, *Int. J. Thermal Sciences*, *71* (2013), Sept., pp. 249 -257

[8] Mohammed, H. A., *et al.*, Heat Transfer Enhancement of Nanofluids in a Double Pipe Heat Exchanger with Louvered Strip Inserts, *Int. Comm. in Heat and Mass Transfer*, *40* (2013), Jan., pp. 36-46

[9] Mukhopadhyay, A., Analysis of Entropy Generation Due to Natural Convection in Square Enclosures with Multiple Discrete Heat Sources, *Int. Comm. in Heat and Mass Transfer*, *37* (2010), 7, pp. 867-872

[10] Shahi, M. M., *et al.*, Entropy Generation Due to Natural Convection Cooling of a Nanofluid, *Int. Comm. in Heat and Mass Transfer*, *38* (2011), 7, pp. 972-983

[11] Khorasanizadeh, H., *et al.*, Numerical Investigation of Cu-Water Nanofluid Natural Convection and Entropy Generation with an Embedded Conductive Baffle, *Scientia Iranica*, *19* (2012), 6, pp. 55-63

[12] Khorasanizadeh, H., *et al.*, Entropy Generation of Cu-Water Nanofluid Mixed Convection in a Cavity, *European Journal of Mechanics B/Fluids*, *37* (2013), Jan.-Feb., pp. 143-152

[13] Cho, C., *et al.*, Natural Convection Heat Transfer and Entropy Generation in Wavy-Wall Enclosure Containing Water-Based Nanofluid, *Int. J. of Heat and Mass Transfer*, *61* (2013), June, pp. 749-758

[14] Cho, C., Heat Transfer and Entropy Generation of Natural Convection in Nanofluid-Filled Square Cavity with Partially-Heated Wavy Surface, *International Journal Thermophysics*, *77* (2014), Oct., pp. 818-827

[15] Wang, Z. L., *et al.*, Thermal-Conductivity and Thermal-Diffusivity Measurements of Nanofluids by 3ω Method and Mechanism Analysis of Heat Transport, *International Journal Thermophysics*, *28* (2007) 4, pp. 1255-1268

[16] Nie, C., *et al.*, Discussion of Proposed Mechanisms of Thermal Conductivity Enhancement in Nanofluids, *International Journal of Heat and Mass Transfer*, *51* (2008), 5-6, pp. 1342-1348

[17] Patel, H. E., *et al.*, A Micro-Convection Model for Thermal Conductivity of Nanofluids, *Journal of Physics*, *65* (2005), 5, pp. 863-869

[18] Wang, X., *et al.*, Heat Transfer Enhancement of CuO-Water Nanouids Considering Brownian Motion of Nanoparticles, *Journal Information & Computational Science*, *9* (2012), 5, pp. 1223-1235

[19] Masoumi, N., *et al.*, A New Model for Calculating the Effective Viscosity of Nanofluids, *Journal Physics*, *42* (2009), 5, pp. 43-51

[20] Ghasemi, B., Aminossadati, S.,M, Brownian Motion of Nanoparticles in a Triangular Enclosure with Natural Convection, *International Journal of Thermal Sciences*, *49* (2010), 6, pp. 931-940

[21] Pakravan, H. A., Yaghoubi, M., Combined Thermophoresis, Brownian Motion and Dufour Effec Its on Natural Convection of Nanofluids, *International Journal of Thermal Sciences*, *50* (2011), 3, pp. 394-402

[22] Arefmanesh, A. *et al.*, Mixed Convection Heat Transfer in a CuO-Water Filled Trapezoidal Enclosure, Effects of Various Constant and Variable Properties of the Nanofluid, *Applied Mathematical Modelling*, *40* (2016), 2, pp. 815-831

[23] Haddad, Z., Abu-Nada, E., Natural Convection in Nanofluids: Are the Thermophoresis and Brownian Motion Effects Significant in Nanofluid Heat Transfer, *Int. J. Thermal Sciences*, *57* (2012), July, pp. 152 -162

[24] Seyf, H. R., Nikaaein, B., Analysis of Brownian Motion and Particle Size Effects on the Thermal Behavior and Cooling Performance of Microchannel Heat Sinks, *Int. J. of Thermal Sciences*, *58* (2012), Aug., pp. 36-44

[25] Bianco, V., *et al.*, Entropy Generation Analysis of Turbulent Convection Flow of Al_2O_3-Water Nanofluid in a Circular Tube Subjected to Constant Wall Heat Flux, *Energy Conversion and Management*, *77* (2014), Jan., pp. 306-314

[26] Bianco, V., *et al.*, Second Law Analysis of Al_2O_3-Water Nanofluid Turbulent Forced Convection in a Circular Cross Section Tube with Constant Wall Temperature, *Advances in Mechanical Engineering 2013*, (2013), ID 920278

[27] Brinkman, H. C. The Viscosity of Concentrated Suspensions and Solution, *Journal Chemical Physics*, *20* (1952), 4, pp. 571-581

[28] Maxwell-Garnett, J. C., Colours in Metal Glasses and in Metallic Films, *Philos. Trans. Roy. Soc. A*, *203* (1904), 359-371, pp. 385-420

[29] Koo, J., Kleinstreuer, C., A New Thermal Conductivity Model for Nanofluids, *Journal Nanoparticle Research*, *6* (2004), 6, pp. 577-588

[30] Vajjha, R. S., Das, D. K., Experimental Determination of Thermal Conductivity of Three Nanofluids and Development of New Correlations, *Int. J. Heat and Mass Transfer*, *52* (2009), 21-22, pp. 4675-4682

[31] Patankar, S. V., *Numerical Heat Transfer and Fluid Flow*, McGraw-Hill, New York, USA, 1980

[32] Chamkhaa, A. J, Abu-Nada, E., Mixed Convection Flow in Single- and Double-Lid Driven Square Cavities Filled With Water-Al_2O^3 Nanofluid: Effect of Viscosity Models, Eur., J*ournal of Mechanics B/Fluids*, *36* (2012), Nov.-Dec., pp. 82-96, 2012